PROCEEDINGS OF SCIENCE

Hadronic resonances in pp and Pb–Pb collisions with ALICE

Enrico Fragiacomo* **(for the ALICE collaboration)**
INFN - Sezione di Trieste, via Valerio 2, Trieste, 34127, Italy
E-mail: enrico.fragiacomo@ts.infn.it

Resonances, with their lifetime comparable to the lifetime of the partonic plasma phase, are a valuable tool to study the dynamics of the high energy density medium formed in heavy-ion collisions. Resonance measurements can be potentially used to estimate the time span between the chemical and kinetic freeze-out and interaction cross sections in the hadronic phase. Measurements of resonances in proton-proton collisions provide an important baseline for heavy-ion data as well for tuning QCD-inspired particle production models. The ALICE collaboration has measured $K^*(892)^0$ and $\phi(1020)$ production in Pb–Pb collisions at $\sqrt{s_{NN}}$ = 2.76 TeV and in pp collisions at $\sqrt{s}$ = 7 TeV. Characteristics of resonance production in these collisions systems will be discussed, in particular transverse momentum spectra and ratios such as ϕ/K and K^{*0}/K. For pp collision data a comparison with QCD inspired models will be shown.

The European Physical Society Conference on High Energy Physics
18-24 July, 2013
Stockholm, Sweden

*Speaker.

PoS(EPS-HEP 2013)174

1. Introduction

Hadronic resonances are a sensitive probe of the dynamical evolution of the fireball since a significant fraction of them decay in the time span (of the order of few fm/c) between chemical and kinetic freeze-out [1, 2, 3]. The measured resonance signal can be reduced by the rescattering of the resonance decay products. Resonances may also be regenerated through collisions of hadrons. The competition between resonance-generating processes and rescattering depends on the lifetime and the temperature of the fireball and determines the ratio of the resonance to non-resonance yields. Particularly interesting is the comparison of ϕ and K^{*0} production, considering the different lifetimes (about a factor 10) of the two resonances. Due to the large lifetime (46 fm/c) the ϕ is expected to decay outside the hot and dense interacting medium. In these proceedings, the resonant-to-stable particle ratios ϕ/K and K^{*0}/K will be presented, providing some hints of a larger rescattering effect on the K^{*0} meson.

Another effect which is expected to show up in the fireball near the phase transition, is a partial restoration of the chiral symmetry. It is predicted [4, 5] that resonances which decay when chiral symmetry is at least partially restored will exhibit mass shifts or width broadening with respect to the vacuum values. Any difference between measured masses and widths in Pb–Pb collisions with respect to those in pp collisions, which in turn are in agreement with the PDG values [6], could be interpreted as a possible signature of restoration of the chiral symmetry.

Results for pp collisions provide the necessary benchmark for studying possible effects of the hadronic medium which affect the measured quantities in Pb–Pb collisions. Beside this goal, the study of resonances in pp collisions contributes to the understanding of hadron production mechanisms and provides a reference for tuning QCD-inspired event generators [6].

The results reported in this proceedings refer to analyses carried out using a sample of 60 (80) million minimum-bias pp data at $\sqrt{s}$ = 7 TeV, for the ϕ (K^{*0}), and a sample of 10 million Pb–Pb data at $\sqrt{s_{\rm NN}}$ = 2.76 TeV, collected with the ALICE detector. Measurements of the $K^*(892)^0$ and $\bar{K}^*(892)^0$ are averaged and these particles are collectively called K^{*0}.

2. Experimental setup and analysis

The ALICE detector [7, 8] is designed to study both pp and Pb–Pb collisions at TeV-scale energies. The detectors used in this analysis include, from the innermost outwards, the Inner Tracking System (ITS), the Time Projection Chamber (TPC) and the Time Of Flight array (TOF). Furthermore, two forward scintillator hodoscopes (VZERO) placed along the beam direction on either side of the interaction point were used for minimum-bias triggering and for rejecting beam-gas interactions. The standard tracking used in this analysis combines the information from the ITS and TPC. The momentum resolution of the TPC is in the range 1-7% for pions with $1 < p_{\rm T} < 10$ GeV/c. Furthermore it provides very good resolution in the distance of closest approach to the vertex (impact parameter resolution in the transverse direction is <100 μm for $p_{\rm T} > 1$ GeV/c) and hence an excellent separation of primary and secondary particles. The TPC also provides particle identification (PID) via dE/dx measurements. The TPC dE/dx measurements allow pions to be separated from kaons for momenta up to $p \sim 0.7$ GeV/c, while the proton/antiproton band starts to overlap with the pion/kaon band at $p \sim 1$ GeV/c. The TOF allows pions and kaons to be unambiguously

identified up to $p \sim 1.5$-2.0 GeV/c. The two mesons can be distinguished from (anti)protons up to $p \sim 2.5$ GeV/c.

Resonances are identified by their main hadronic decay channel ($K^{*0} \longrightarrow \pi^{\pm}\ K^{\mp}$ and $\phi \longrightarrow K^{+}\ K^{-}$). Due to their very short lifetimes, decay products cannot be distinguished from particles coming from the primary vertex. Their yield is obtained by computing the invariant mass spectrum of all primary candidates and then subtracting a combinatorial background. This was performed by either the event-mixing or the like-sign technique. The signal, after subtracting the combinatorial background, was then fitted with a Breit-Wigner plus a polynomial for the residual background. A Voigtian function (convolution of Breit-Wigner function and Gaussian) was used for the extraction of the ϕ raw yield. Some examples of invariant mass spectra are presented in Figures 1 and 2.

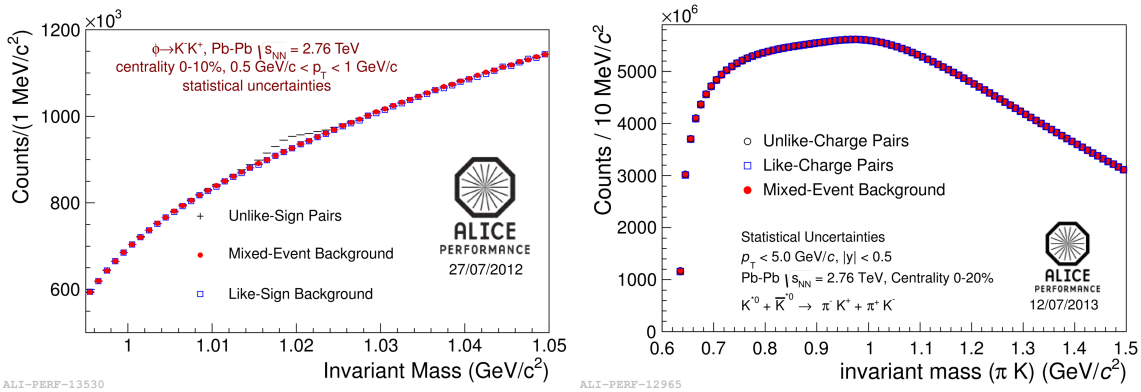

Figure 1: The $K^{+}K^{-}$ ($\pi^{\pm}K^{\mp}$) invariant mass distribution in Pb–Pb collisions at $\sqrt{s_{\rm NN}}$ = 2.76 TeV.

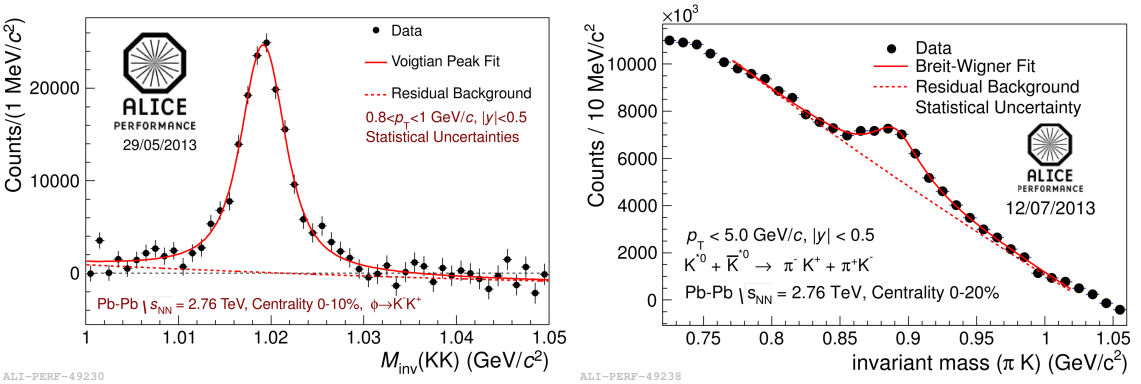

Figure 2: The $K^{+}K^{-}$ ($\pi^{\pm}K^{\mp}$) invariant mass distribution in Pb–Pb collisions at $\sqrt{s_{\rm NN}}$ = 2.76 TeV after the subtraction of the mixed-event background. The fitting function is the sum of a Voigtian (Breit-Wigner) function and a polynomial.

In order to extract the total production yield, the raw counts were corrected for the decay branching ratio and for the losses due to geometrical acceptance and detector efficiency. These were determined by Monte Carlo simulation, with particle production simulated using PYTHIA [9] or HIJING [10], for pp and Pb–Pb data respectively, and interactions with the ALICE detector simulated using GEANT3 [11].

Final yields were obtained normalizing to the number of inelastic collisions (pp collisions) or to the number of analyzed events in a given centrality range (Pb–Pb collisions). The trigger efficiency was also taken into account. The analyses of K^{*0} and ϕ mesons in pp collisions at $\sqrt{s}$ = 7 TeV are described in detail in [6].

3. Results

Figures 3 and 4 show the masses and the widths as functions of p_T for the ϕ and the K^{*0} in Pb–Pb collisions at $\sqrt{s_{NN}}$ = 2.76 TeV. All the measured values are in agreement with the PDG values, as it was measured in pp collisions [6]. For the ϕ, results for two different centrality bins are presented, which also exclude any centrality dependence of mass and width. For the K^{*0} the comparison with Monte Carlo (HIJING) predictions is also shown.

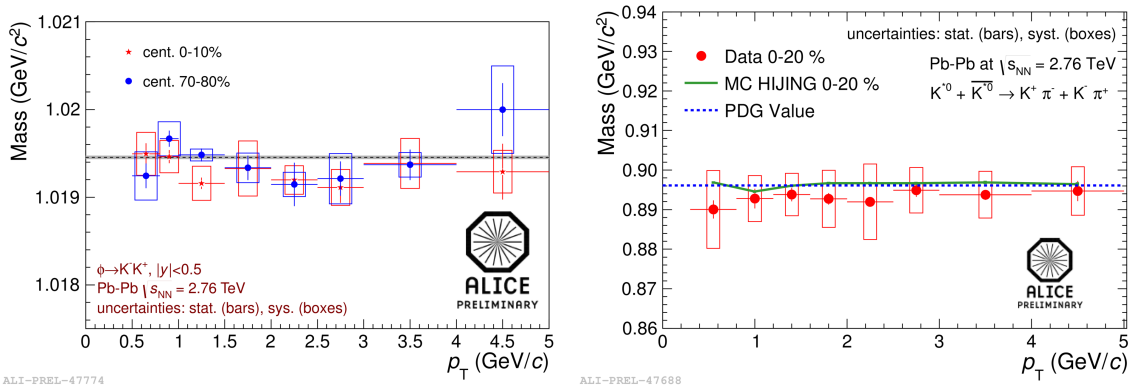

Figure 3: Mass of ϕ and K^{*0} in Pb–Pb collisions at $\sqrt{s_{NN}}$ = 2.76 TeV. For the ϕ, results for two different centrality bins are presented. No mass shift is observed.

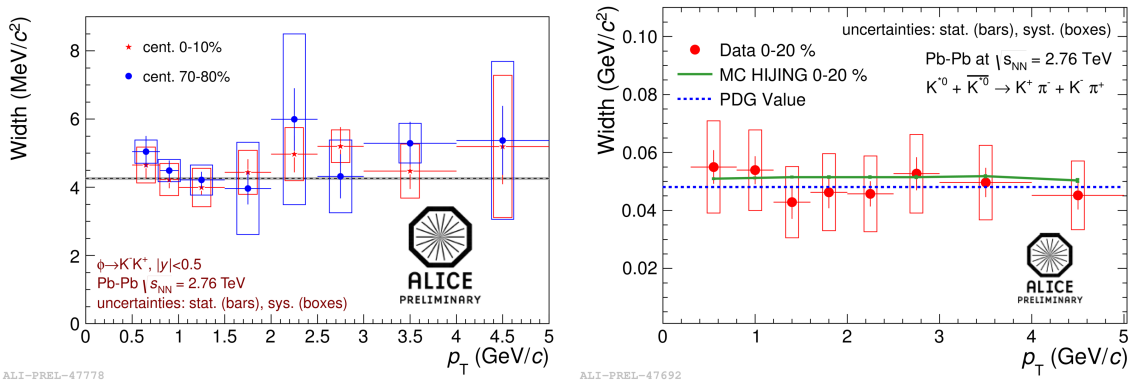

Figure 4: Width of ϕ and K^{*0} in Pb–Pb collisions at $\sqrt{s_{NN}}$ = 2.76 TeV. For the ϕ, results for two different centrality bins are presented. No width broadening is observed.

3.1 Results in pp collisions at $\sqrt{s}$ = 7 TeV

Figure 5 shows the K^{*0} and ϕ p_T-spectra with a comparison to a number of PYTHIA tunes [9] and PHOJET [13]. The best agreement is found for the recent PYTHIA Perugia 2011 tune,

although only the high-p_{T} part ($p_{\mathrm{T}} > 3$ GeV/c) of the ϕ spectrum is reproduced. A good agreement is found for the K^{*0}.

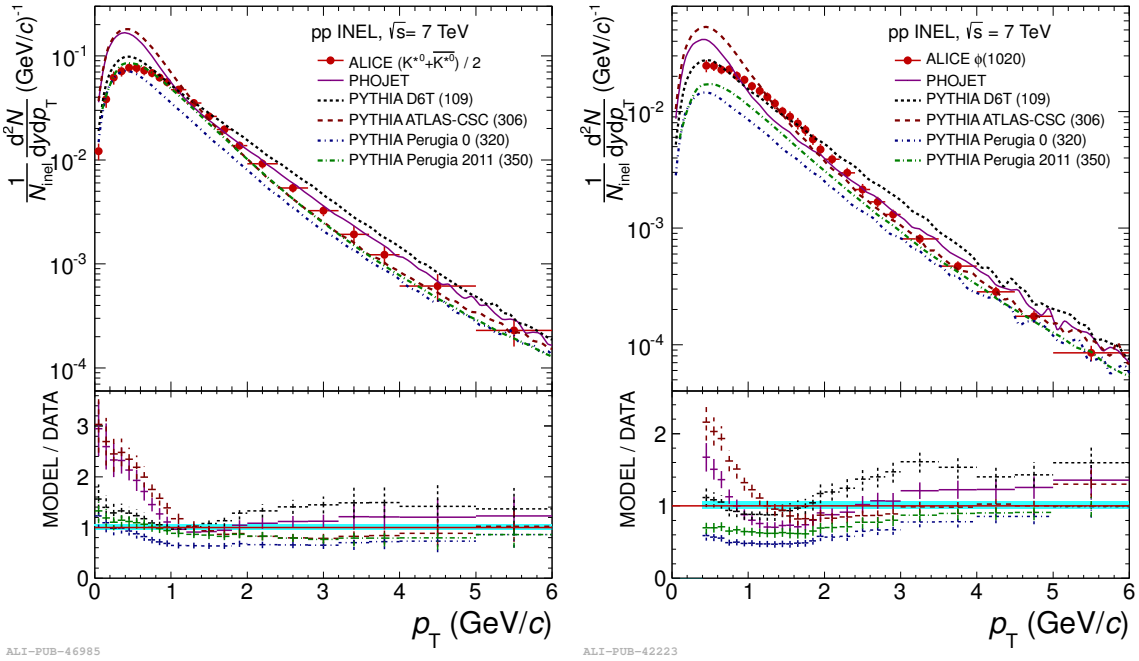

Figure 5: Comparison of K^{*0} and ϕ p_{T}-spectra in inelastic pp collisions at $\sqrt{s} = 7$ TeV with PHOJET and PYTHIA tunes [12].

3.2 Results in Pb–Pb collisions at $\sqrt{s_{\mathrm{NN}}}$ = 2.76 TeV

Figure 6 shows the K^{*0} and ϕ p_{T}-spectra fit with Boltzmann-Gibbs Blast-Wave functions [14]. The resonance spectra are integrated to give the particle yield, $\mathrm{d}N/\mathrm{d}y$, with the spectrum fits used to estimate the resonance yields at low and high p_{T}, where no signals could be measured.

Figure 7 (left) shows the resonance to kaon yield ratios as a function of centrality (K^- yields from [15]). An hint of decrease for the $\mathrm{K}^{*0}/\mathrm{K}^-$ ratio is observed from peripheral to central Pb–Pb collisions. This suppression of the $\mathrm{K}^{*0}/\mathrm{K}^-$ ratio in central collisions may be due to rescattering effects. The same trend is not seen for the ϕ/K^- ratio which is independent of the collision centrality and consistent with the values measured in pp collisions. This seems to suggest that the ϕ yield is little affected by rescattering effects which is consistent with the longer lifetime of the ϕ (46 fm/c) with respect to the K^{*0} (4 fm/c).

Figure 7 (right) shows the $\mathrm{K}^{*0}/\mathrm{K}^-$ ratio as a function of $\sqrt{s_{\mathrm{NN}}}$ for different collision systems. At both RHIC and LHC energies, the $\mathrm{K}^{*0}/\mathrm{K}^-$ ratio is the same in pp collisions but decreases in heavy-ion collisions with an effect which is at least as large at the LHC energies. This effect could again be related to the interaction of the daughters with the hadronic medium which affects the K^{*0} yield (and not the ϕ) due to its shorter lifetime.

4. Conclusions

The hadronic resonances $\mathrm{K}^*(892)^0$ and $\phi(1020)$ have been measured in pp collisions at $\sqrt{s} = 7$ TeV

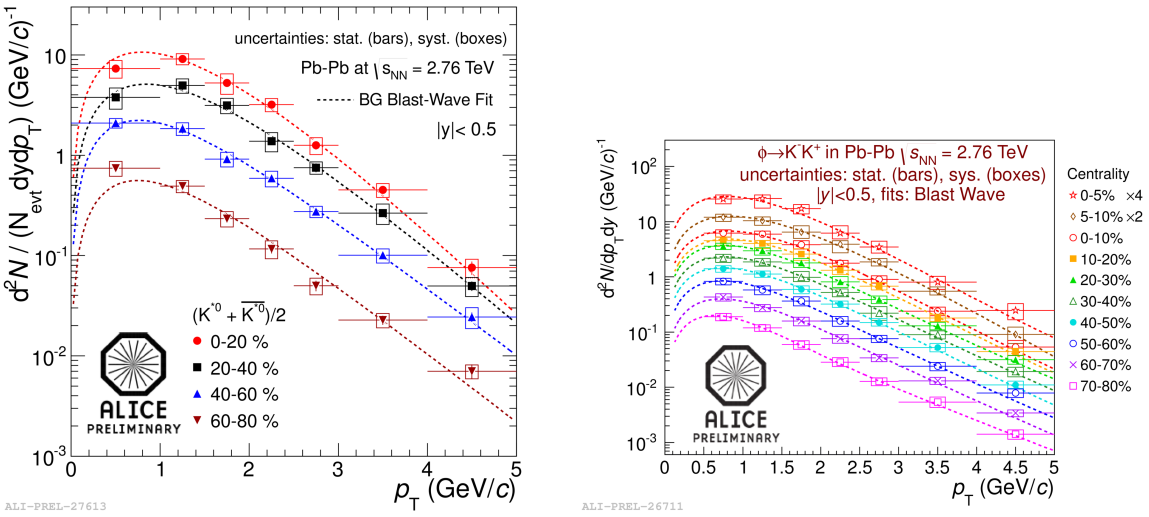

Figure 6: K^{*0} and ϕ p_T-spectra in Pb–Pb collisions at $\sqrt{s_{NN}}$ 2.76 TeV in different centrality classes.

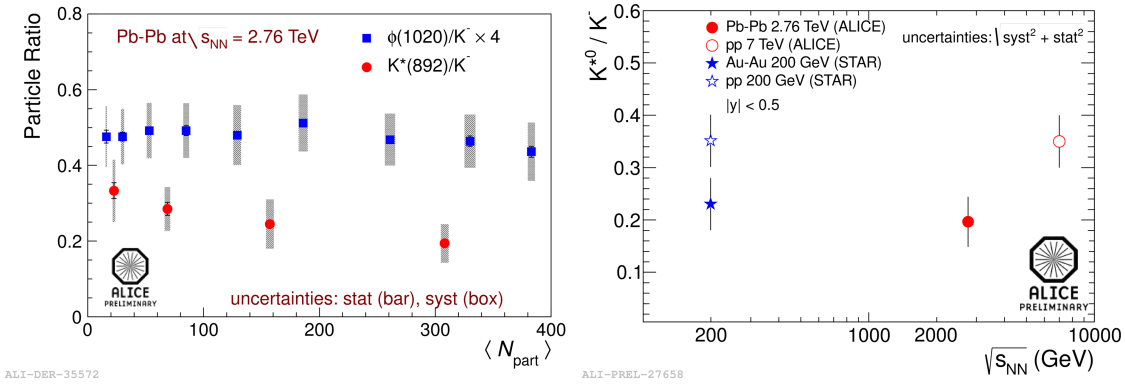

Figure 7: (Left) K^{*0}/K^{-} and ϕ/K^{-} ratios as a function of centrality. (Right) K^{*0}/K^{-} ratio as a function of $\sqrt{s_{NN}}$ for different collision systems. STAR values from [16]. ALICE pp values from [6].

and in Pb–Pb collisions at $\sqrt{s_{NN}}$ = 2.76 TeV for different event centrality bins with the ALICE detector at the LHC. Transverse momentum spectra of K^{*0} and ϕ measured in pp collisions have been compared to PHOJET and different PYTHIA tunes. Only the K^{*0} is reproduced by Perugia 2011 PYTHIA tune. The masses and the widths of the K^{*0} and ϕ resonances reconstructed via hadronic decays in Pb–Pb collisions are consistent with the vacuum values. The K^{*0}/K and ϕ/K ratios are independent of $\sqrt{s_{NN}}$ from RHIC to LHC energies. The K^{*0}/K ratio is higher in pp collisions than in A–A collisions at RHIC and LHC energies. While the ϕ/K ratio is independent of collision centrality, the K^{*0}/K ratio shows an hint of decrease with increasing centrality, suggesting that rescattering effects cause a reduction in the measurable K^{*0} signal in central collisions.

References

[1] M. Bleicher and J. Aichelin, Phys. Lett. B **530** (2002) 81

[2] M. Bleicher and H. Stocker, J. Phys. G **30** (2004) S111-8

[3] C. Markert, G. Torrieri and J. Rafelski, Proc. of PASI 2002, hep-ph/0206260

[4] G.E. Brown and M. Rho, Phys. Rep. **363** (2002) 85

[5] R. Rapp, J. Wambach and H. van Hees (2009), arXiv: 0901.3289v1

[6] B. Abelev, et al., ALICE Collaboration, Eur. Phys. J. C **72** (2012)

[7] K. Aamodt, et al., ALICE Collaboration, J. Instr. **3** (2008) S08002

[8] K. Aamodt, et al., ALICE Collaboration, J. Instr. **5** (2010) P03003

[9] T. Sjöstrand, S. Mrenna and P. Skands, J. High Energy Phys. **05** (2006) 026

[10] X.N. Wang and M. Gyulassy, Phys. Rev. D **44** (1991) 3501

[11] R. Brun, F. Carminati and S. Giani, CERN-W5013

[12] B. Abelev, et al., ALICE Collaboration,Eur. Phys. J. C **72** (2012) 2183.

[13] R. Engel, et al., Z. Phys. C **66** (1995) 203; R. Engel and J. Ranft, Phys. Rev. D **54** (1996) 4244

[14] E. Schnedermann, J. Sollfrank and U. Heinz, Phys. Rev. C **48** (1993) 2462

[15] B. Abelev, et al., ALICE Collaboration, CERN-PH-EP-2013-019, arXiv:1303.0737v2

[16] M.M. Aggarwal, et at., STAR Collaboration, Phys. Rev. C **84** (2011) 034909

PoS(EPS-HEP 2013)174